Neuroscience 285 (2015) 303–311

SPECTROSCOPIC MEASUREMENT OF CORTICAL NITRIC OXIDE RELEASE INDUCED BY ASCENDING ACTIVATION

N. ESPINOSA,* J. CUDEIRO AND J. MARIÑO

Laboratory of Neuroscience and Motor Control (NEUROcom), Department of Medicine-INEF-Galicia, University of A Coruña and Institute of Biomedical Research (INIBIC), 15006 A Coruña, Spain

Abstract—The transition from sleep to the awake state is regulated by the activation of subcortical nuclei of the brainstem (BS) and basal forebrain (BF), releasing acetylcholine and glutamate throughout the cortex and inducing a tonic state of neural activity. It has been suggested that such activation is also mediated by the massive and diffuse cortical release of nitric oxide (NO). In this work we have combined the spectroscopic measurement of NO levels in the somatosensory cortex of the cat through its marker methemoglobin, as well as two other hemodynamic markers (oxyhemoglobin – oxyHb – and deoxyhemoglobin – deoxyHb), together with the electrical stimulation of BS and BF – to induce an experimental transition from a sleep-like state to an awake-like mode. The results show an increase of NO levels either after BS or BF activation. The response induced by BS stimulation was biphasic in the three studied markers, and lasted for up to 30 s. The changes induced by BF were monophasic lasting for up to 20 s. The systemic blockade of NO production abolished the observed responses to BS whereas responses to BF stimulation were much less affected. These results indicate a crucial role for NO in the neuronal activation induced by the ascending systems.

Key words: hemodynamics, sleep, somatosensory cortex, spectroscopy.

INTRODUCTION

Arousal is the consequence of an orchestrated change in cortical and subcortical structures. The transition from sleep to the awake state is mainly induced by brainstem (BS) and basal forebrain (BF) neurons (Steriade et al., 1993a), which are part of the classic activating ascending system. As a result of such activation, the cortical release of acetylcholine (ACh) and glutamate (Glu) disrupts the sleep slow oscillatory activity and promotes a transition to the characteristic tonic state of the awake brain (for a review see Steriade et al., 1997). It has been suggested that nitric oxide (NO) is also an important actor in this activation, mainly through its release by cholinergic BF neurons sending axons to the cortex (Bickford et al., 1994; Cudeiro et al., 2000) and by cortical nitrergic neurons (Cudeiro et al., 1997).

Brain sleep mechanisms have been extensively studied using anesthetized cats as a model to reproduce the slow-wave sleep and its dynamics (Steriade et al., 1991a,b; McCormick and Bal, 1997). Also, under experimental conditions, the global cortical activity can be efficiently modified through microstimulation of either the peribrachial region (PBr; Moruzzi and Magoun, 1949; Francesconi et al., 1988; Hartveit et al., 1993; Uhlrich et al., 1995; Wolfe and Palmer, 1998), located in the BS, or the nucleus basalis of Meynert (NB; Metherate et al., 1992; Mariño and Cudeiro, 2003), located in the BF. The BS contains cholinergic, nitrergic and catecholaminergic neurons sending axons to BF and the thalamus (Steriade et al., 1988). BF neurons extensively release ACh throughout the cortex and, as indicated, probably NO, while thalamocortical neurons release Glu. In the anesthetized cat, the activation of such systems has been proved to be a useful tool to study the sleep–wake mechanisms (Steriade et al., 1991b; Li et al., 1999; Mariño and Cudeiro, 2003).

We have previously shown that the systemic and local blockade of NO synthesis (by 7-nitroindazole and L-NOArg respectively) reduces the tonic activation of cortical neurons after subcortical stimulation (Mariño and Cudeiro, 2003). Nonetheless, as far as we know, no direct measurements of that supposed massive NO release has been reported yet. Here, using intracortical spectroscopy in the somatosensory cortex (SSC), we have measured the *in vivo* dynamics of cortical NO levels during sleep-like slow oscillatory activity (induced by anesthesia) and after the activation induced by BS and BF regions, together with the measurements of two hemodynamic markers, oxyhemoglobin (oxyHb) and deoxyhemoglobin (deoxyHb). Our central hypothesis was that, during the intense activation induced by the ascending systems, there is a diffuse and acute production of neuronal NO in the cortex, thus collaborating in the transition from sleep to the wake state.

*Corresponding author. Address: Laboratorio de Circuitos Neuronales, Centro de Investigaciones Médicas, Marcoleta 391, Santiago, Chile.
E-mail address: nespinosa@udc.es (N. Espinosa).

Abbreviations: ACh, acetylcholine; BF, basal forebrain; BOLD, blood oxygenation level dependent; BS, brainstem; deoxyHb, deoxyhemoglobin; ECoG, electrocorticogram; Glu, glutamate; LFi, low-frequency index; metHb, methemoglobin; MR, magnetic resonance; NB, nucleus basalis; nNOS, neuronal nitric oxide synthase; NO, nitric oxide; oxyHb, oxyhemoglobin; PBr, peribrachial region; SSC, somatosensory cortex.

http://dx.doi.org/10.1016/j.neuroscience.2014.11.028
0306-4522/

EXPERIMENTAL PROCEDURES

Experimental preparation

Experiments were performed on 4 adult cats of either sex. Anesthesia was induced with ketamine (15 mg/kg – Pfizer, Madrid, Spain) and xylazine (3 mg/kg – Sigma-Aldrich, Madrid, Spain) i.m. and maintained with isoflurane (1.5–2% for surgery, and 0.5–1% for maintenance, Abbot) in nitrous oxide (70%) and oxygen (30%). Animals were paralyzed with gallamine triethiodide (loading dose of 40 mg, maintenance 10 mg/kg/h i.v., SIGMA) and artificially ventilated; the end tidal CO_2 concentration was adjusted to 3.8–4.2%, body temperature was maintained at 37–38 °C, and heart rate was continuously monitored. Animals were suspended on a stereotaxic frame and the pressure points were infiltrated with lidocaine. The level of isoflurane was chosen to achieve a state of deep anesthesia and particular care was taken to keep a stable pattern of delta (1–4 Hz) slow oscillatory activity throughout the entire experiment. Three craniotomies were performed to insert optical fibers and bipolar tungsten electrodes (details below). All exposed cortical surfaces were bathed in saline to prevent desiccation. At the end of experiments animals were killed by an anesthetic overdose. All animal work was conducted according to national and international guidelines (Spanish Physiology Society and the European Communities Council Directive of November 24, 1986 (86/609/EEC)). The study was approved by the University of A Coruña Ethics Committee (CE-UDC30/1/09).

Electrophysiological and spectroscopy recordings

Electrical and spectroscopic measurements were obtained simultaneously in the primary SSC (S1; coordinates: anterior, 21–23; lateral, 8–10) at a depth of 1–1.5 mm. Electrocorticogram (ECoG) in S1 was continuously recorded and stored (Plexon Inc, Dallas, TX, USA) through a bipolar and concentric electrode at a sampling rate of 2 kHz and filtered on-line with a band-pass of 0.1–500 Hz analog filter (A-M Systems, model 1700).

The method to monitor NO lays in the fact that NO reacts with oxyHb to form methemoglobin (metHb). Thus, metHb levels are proportional to the concentration of NO and can be used as a surrogate marker of such substance (Feelisch et al., 1996; Kelm et al., 1997, González-Mora et al., 2002; Rivadulla et al., 2011). According to this, we used spectroscopy to record the levels of metHb as well as oxy- and deoxyHb. Spectroscopic signals were obtained using two optical fibers (model FCB-UV 100-3-2SMA; diameter 100 μm) arranged in parallel and attached to the electrode. Distance from the electrode tip to the fibers end (located slightly below, see Fig. 2E) was between 100 and 200 μm. Light in the range of 600–700 nm from a halogen lamp was passed through one of the optical fibers and the scattered light was collected by the other. Output was directed to a linear CCD detector (Ocean Optics, Eerbeek, Netherlands) via a compact built-in monochromator and sampled at a rate of 100 Hz with steps of 0.35 nm in the wavelength domain.

To convert the sample intensity recordings S to absorbance values the protocol was as follows: with the fibers located in the tissue, the emitted light was turned off and the dark intensity D was recorded. Next, light was turned on and the reference intensity R was recorded. Then, for a sample intensity at wavelength λ and recorded at time t, $S_\lambda(t)$, the corresponding absorbance, $A_\lambda(t)$, was calculated using the following equation:

$$A(t)_\lambda = -\log_{10}\left(\frac{S(t)_\lambda - D_\lambda}{R_\lambda - D_\lambda}\right) \quad (1)$$

where D_λ and R_λ are the dark and reference intensities for a wavelength λ respectively. Because absorbance is a dimensionless parameter, the value is expressed in arbitrary units (AU).

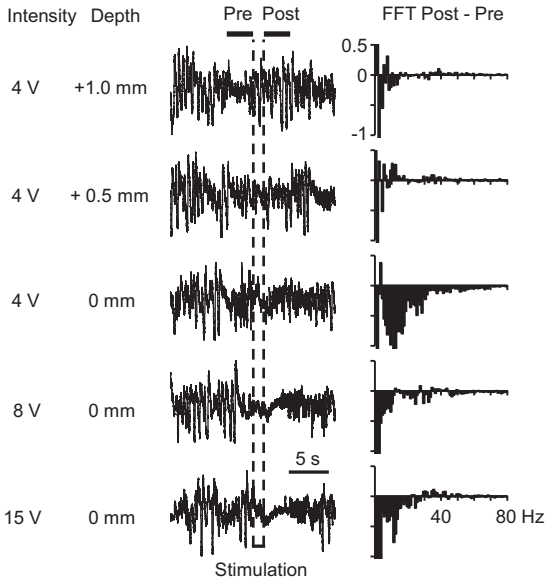

Fig. 1. Electrical stimulation effect obtained for different stimulation intensities and electrode distances from the stereotaxic position (0 mm) of the parabrachial region of BS. Both ECoG wave (left) and its power spectral density (right) reveal changes in low-and high-frequency components. The analysis included the 5 s prior stimulation (Pre), and the 5 s after stimulation (Post). See ''Experimental procedure'' section for details.

Subcortical stimulation and cortical activity modulation

The global cortical activity was efficiently modulated – as indicated by the ECoG recordings – by the combination of anesthesia and electrical stimulation. The continuous anesthetic administration maintained a slow oscillatory pattern within the delta range (Fig. 1, left part of the ECoGs). The temporal transition to an awake-like pattern was achieved through the application of electrical stimulation either in BS or BF (sequentially and randomly through electrical microstimulation at intervals of 2–8 min). Trains of rectangular cathodal shocks (0.05 ms, 0.1–1 mA) were delivered at a frequency of 50 Hz for a period of 2 s through bipolar electrodes (insulated except for 500 μm at the tip; contacts separated by 500 μm). Electrodes were positioned and held in place following a procedure published elsewhere (Mariño and Cudeiro 2003). It allowed us to precisely localize the subcortical loci

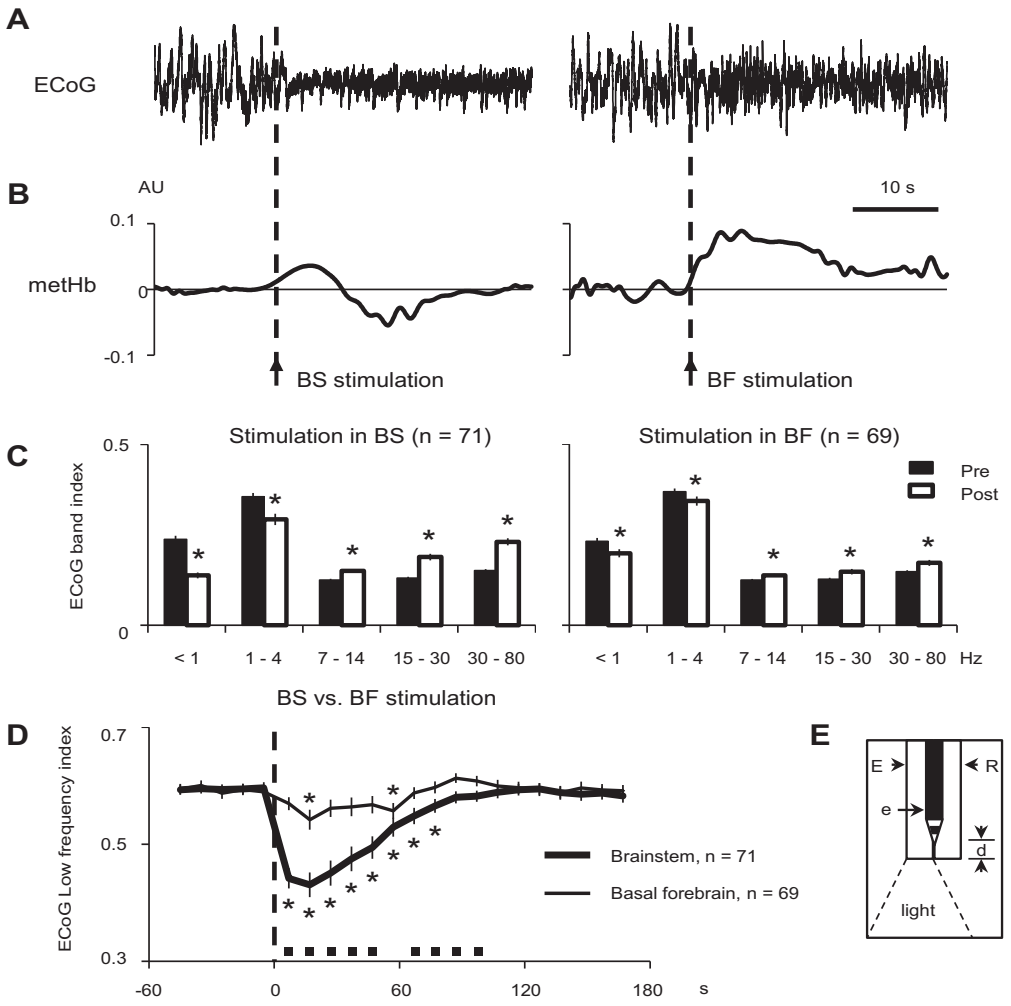

Fig. 2. (A) ECoG activity recorded in S1 before and after electrical stimulation of BS and BF in one cat. (B) Cortical metHb dynamics simultaneously recorded. *Y* axis is the relative concentration of metHb obtained by solving Eq. (4) and expressed in arbitrary units (AU). (C) $ECoG_{index}$ for frequency bands of interest before (solid bars) and after (open bars) electrical stimulation in BS and BF. Recordings were performed in four cats. (D) Low-frequency index analysis. For each brain structure studied, values (mean and SEM) at Post were contrasted with the values Pre stimulation. Dashed line indicates stimulation. Each time-point represents bins of 10 s. Asterisks indicate significant effects at different time points compared to the Pre values. Black squares represent significant differences in the response observed in the two structures at different time-points after the stimulation. E) Schematic drawing of the bipolar tungsten electrode (e) and optical fibers. Emitter (E) and the receiver (R) fibers deliver and collect the light respectively. Distance from the electrode tip to the fibers end (d) was set to 100–200 μm.

for electrical stimulation rendering histological reconstruction, in this case, unnecessary. The procedure was as follows. Horsley–Clarke coordinates were used to achieve the PBr region in the BS (anterior, 0; lateral 4; ventral, −2) and the NB in the BF (anterior, 10–13; lateral, 8.5–10; ventral, −1 to 0). For each electrode, the final position in the vertical axes was adjusted monitoring the stimulation effect on the ECoG activity. Fig. 1 depicts one example of the successive ECoG recordings and frequency spectra obtained during the descent of one stimulating electrode toward the PBr region. A low-intensity (typically 4 V) 2-s train was delivered to localize the optimal position inside each brain region. The search procedure started with the electrode located 4 mm above the theoretical stereotaxic coordinates and the location was tested in steps of 0.25 mm. Once a clear effect on the ECoG was evoked, the voltage was adjusted (between 4 and 15 V) to the minimum intensity capable of optimally inducing a low-amplitude and high-frequency activity in S1 (see waveforms and fast Fourier transform (FFT) analysis in Fig. 1). The same procedure was applied to locate the appropriate stimulating location in the BF. Such effective modulation of the ECoG was indicative of a suitable stimulation of the ascendant pathways (Mariño and Cudeiro 2003).

3.4. Pharmacology

In order to inhibit the enzyme neuronal NOS (neuronal nitric oxide synthase), responsible of neuronal NO production, 7-nitroindazole (7NI; SIGMA) was administered i.v. over 15 s (3.5 mg/kg dissolved in 0.1 ml DMSO (SIGMA); de Labra et al., 2009).

3.5. Data analysis

The FFT was used to obtain the power spectral density from ECoG recordings for periods of 5–10 s before and

after electrical stimulation. Frequency ranges of interest were adjusted to previously described cat sleep rhythms (for a short review, see Steriade et al. (1993b)) according to the following classification: < 1 Hz (slow), 1–4 Hz (delta), 7–14 Hz (spindle), 15–30 Hz (beta) and 30–80 Hz (gamma). To evaluate the electrical stimulation effect on each frequency band, an ECoG index was defined as follows:

$$\mathrm{ECoG}_{\mathrm{index}}(f_n) = \frac{\sum \mathrm{PSD}(f_n)}{\sum \mathrm{PSD}(f_T)} \tag{2}$$

where $\sum \mathrm{PSD}(f)$ is the cumulative sum of the power spectral density for the frequency range f. f_n is the frequency range for one of the rhythms aforementioned and f_T is the frequency range between 0 and 80 Hz (DC component filtered previously). Specifically, to evaluate the power of the lowest frequency waves in the ECoG, a low-frequency index (LFi) was defined as follows:

$$\mathrm{LFi} = \frac{\sum \mathrm{PSD}(f_L)}{\sum \mathrm{PSD}(f_T)} \tag{3}$$

where f_L is the frequency range below 4 Hz.

For the spectroscopic recordings, absorbance values were filtered (Savitzky–Golay filter) and linearly interpolated in the wavelength domain (range 600–700 nm, steps of 1 nm) and in time domain to normalize timestamps (100 Hz, $t = 0$ s for the electrical stimulation onset). The relative concentration of oxyHb, deoxyHb and metHb were calculated by means of the Lambert–Beer's law solving the following Eq. (4).

$$\begin{bmatrix} \Delta\mathrm{oxyHb}(t) \\ \Delta\mathrm{deoxyHb}(t) \\ \Delta\mathrm{metHb}(t) \end{bmatrix} = \begin{bmatrix} \alpha_{\mathrm{oxyHb}}^{\lambda_1} \alpha_{\mathrm{oxyHb}}^{\lambda_2} \alpha_{\mathrm{oxyHb}}^{\lambda_3} \\ \alpha_{\mathrm{deoxyHb}}^{\lambda_1} \alpha_{\mathrm{deoxyHb}}^{\lambda_2} \alpha_{\mathrm{deoxyHb}}^{\lambda_3} \\ \alpha_{\mathrm{metHb}}^{\lambda_1} \alpha_{\mathrm{metHb}}^{\lambda_2} \alpha_{\mathrm{metHb}}^{\lambda_3} \end{bmatrix} \cdot \begin{bmatrix} A_{\lambda_1}(t) \\ A_{\lambda_2}(t) \\ A_{\lambda_3}(t) \end{bmatrix} \tag{4}$$

where $\alpha_{\mathrm{oxyHb}}^{\lambda_i} \alpha_{\mathrm{deoxyHb}}^{\lambda_i}$ and $\alpha_{\mathrm{metHb}}^{\lambda_i}$ are the extinction spectra, at wavelength λ_i, for oxy-, deoxy-, and metHb, respectively. Since $A_{\lambda_i}(t)$ is the recorded absorbance value at wavelength λ_i (see Eq. (1)), we solved Eq. (4) for different wavelength trios selected randomly within the range 600–700 nm (steps of 1 nm; smaller steps did not modified the statistical significance of final results) until the whole wavelength range was covered. The extinction spectra reported by Zijlstra et al. (2000) was used for the corresponding wavelengths. As a result, for each relative concentration we obtained a distribution and the average value was taken as the estimated value at time = t. Finally, a wavelet filter was applied to oxy-, deoxy-, and metHb in the time domain using a family of Meyer (discrete approximation) wavelets.

Statistical analysis was done using paired t-test or Wilcoxon test. The hypothesis of normality was checked using the Kolmogorov–Smirnov test. Results were deemed to be significant when $p < 0.05$. Both analytical and statistical analyses were performed using in-house software written in MATLAB (MathWorks, 2010).

RESULTS

Effects on ECoG activity of the electrical stimulation of activating ascendant pathways

The sleep-like ECoG activity induced by anesthesia was modified by the electrical stimulation of BS and BF (Fig. 2A). The ECoG changed from a high-amplitude low-frequency pattern of activity to a low-amplitude high-frequency mode.

Electrical stimulation of BS ($n = 71$) and BF ($n = 69$) modified the sleep-like oscillatory activity induced by anesthesia in different ways. To quantify this phenomenon, the ECoG power spectral density was calculated 5 s before the onset and 5 s immediately after the offset of the electrical stimulation. The $\mathrm{ECoG}_{\mathrm{index}}$ in the frequency of interest bands were calculated (see "Experimental procedure" section). Population analysis of the effects induced by BS (Fig. 2C, left) and BF (Fig. 2C, right) stimulation revealed a decrease in the low-frequency activity (below 4 Hz) and an increase of higher frequency components (above 4 Hz).

To analyze the persistence and strength of the electrical stimulation effects, the LFi (see "Experimental procedure" section) was calculated using 10-s bins. Fig. 2D reveals a fast drop of the LFi induced by BS activation, lasting for up to 60 s after the electrical stimulation, whereas BF stimulation induced significant changes 10 s after the stimulation and lasting only 10 s (with an apparent late rebound). Besides, not only the duration but also the magnitude of the effects induced on the ECoG by the electrical stimulation on BS and BF was different (the statistically significant differences are indicated by black squares in Fig. 2D).

Effects on NO and hemodynamic markers of the stimulation of ascending pathways

Spectrometric recordings simultaneous to the above-mentioned ECoG, revealed that those changes were accompanied by a patent increase in cortical metHb (Fig. 2B). Population analysis of the time course of changes in met-, deoxy-, and oxyHb induced by BS and BF stimulation is show in Fig. 3. To define statistical variations, the mean values during control condition, i.e. before the electrical stimulation, were compared with each value after the stimulation (paired t-test). The resulting time intervals with significant changes are shown by marks below the curves.

Stimulation in BS (thick curves in Fig. 3) induced an increase of metHb, followed by a subsequent decrease, lasting in total for up to 30 s after the stimulation (as indicated by the reference lines below the curve). A similar biphasic change, but in the opposite direction, was observed for the deoxyHb. Changes in of oxyHb were less conclusive, showing an initial increase of its levels lasting for around 10 s after the stimulation, followed by a variable – although in some periods statistically significant – response.

With regard to BF stimulation (thin curves in Fig. 3), it induced, in contrast, a monophasic variation of the three markers. The mean response showed a clear increase of metHb levels, lasting for around 20 s after the

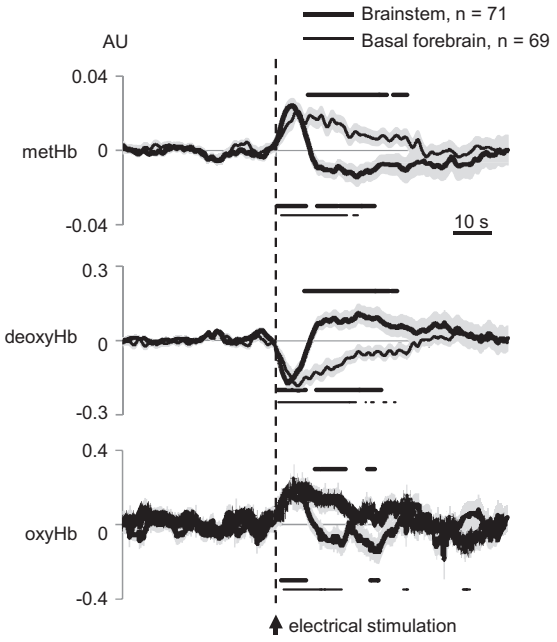

Fig. 3. BS and BF stimulation-induced responses at S1 on the three studied markers. Dots under curves show significant changes at different time-points after BS (thick dots) and BF (thin dots) stimulation compared to the average response 60 s before the stimulation. Dots above curves denote significant differences between temporal profiles for BS and BF stimulation. Shaded area represents SEM. Values obtained by solving Eq. (4) and expressed in arbitrary units (AU). Recordings were performed simultaneously with ECoGs analyzed in Fig. 2C, D (four cats).

stimulation; together with a decrease of deoxyHb and an increase of oxyHb of similar duration.

Finally, statistical comparison between the responses obtained with BS and BF stimulation revealed that both hemodynamic markers and metHb showed the same temporal pattern during the first 10 s after the end of the electrical stimulation.

Dissecting the role of NO on cortical activation

As we had previously shown, the systemic application of 7NI reduced the efficacy of the ascendant activation to modify the ECoG slow pattern (Mariño and Cudeiro, 2003). In the present study we compared that phenomenon with the simultaneously recorded spectroscopic measurements.

The spectroscopic measurements allowed us to precisely follow the NO levels before and after 7NI injection. Fig. 4A shows the post-stimulus dynamics (average, $n = 5$) of cortical metHb after BS and BF stimulation during control condition (top panel), peak drug effect (middle panel) and recovery from nNOS inhibition (bottom panel). To compare the metHb responses induced by stimulation, the resting value – mean value 40 s before electrical stimulation – was subtracted from each curve (see Fig. 4C). To quantify the effect of 7NI on NO as well as on the two hemodynamic markers, and having into account the specific time course of each response, the stimulation evoked responses were integrated for BS (10 s interval post stimulus) and BF (30 s interval post stimulus) (Fig. 4B; intervals α depicted in Fig. 4A). After 7NI administration there was a clear impairment in the ability of the ascending activation to modify oxy-, deoxy- and metHb levels, mainly during 11–20 min after 7NI application. In addition, the electrical activity during this period contains a higher component on the low-frequency band (Fig. 4B bottom panel). It is interesting to note that the resting values of the measured substances, but not the ECoG, were also affected by the nNOS blockade (Fig. 4C). Similarly to the observed effects on the evoked responses, these changes lasted for up to 20 min.

DISCUSSION

The present study unveils the *in vivo* changes on NO dynamics in the cat cortex during the transition from a global pattern of synchronized slow activity to an awake-like mode. In previous works we suggested a direct role for the neuronal NO in the cortical activation induced by the ascending systems. We observed that the changes in ECoG activity induced by BF stimulation were practically abolished when administering 7NI i.p. (Mariño and Cudeiro, 2003). Here, by means of spectroscopic continuous recordings, we have studied in detail the time course of NO release, and compared it with the responses induced by BF and BS stimulation.

Our results show that, in parallel to the categorical disruption of the slow ECoG activity evoked by BS and BF stimulation, there is an increase of NO levels immediately after the activation, lasting for 10 s (BS) or 20 s (BF). This fact strongly supports our hypothesis that the sudden and global release of NO throughout the cortex (we have measured a similar NO dynamics in primary visual cortex; not shown here) is directly contributing to the characteristic neuronal activation that occurs during the transition from slow to tonic activity. In the present work the spontaneous slow delta activity was induced by anesthesia, and cortical de-synchronization was transiently evoked by electrical stimulation; but the observed NO changes are likely to be of similar nature under natural sleep–wake transitions. The magnitude of the referred changes was smaller in metHb than in the other markers (note arbitrary unit axes in Fig. 3). It must be noted that BF stimulation evoked significant changes of shorter duration, an effect than can explain the smaller changes observed in the ECoG after this activation. An interesting possibility to complement our data could be the use of imaging techniques (e.g. optical imaging). It might provide spatial information to corroborate the ‘‘diffuse’’ increase in NO over the cortex. Certainly it will deserve attention in future experiments together with multiple spectroscopic measurements on different cortical areas.

Is this NO-mediated cortical activation dependent on cGMP production? Our experimental approach does not allow us to directly address this issue and we can only speculate. In the cerebral cortex, the diversity of NO production sites suggests a complex role in cortical processing and perhaps more than a single mode of

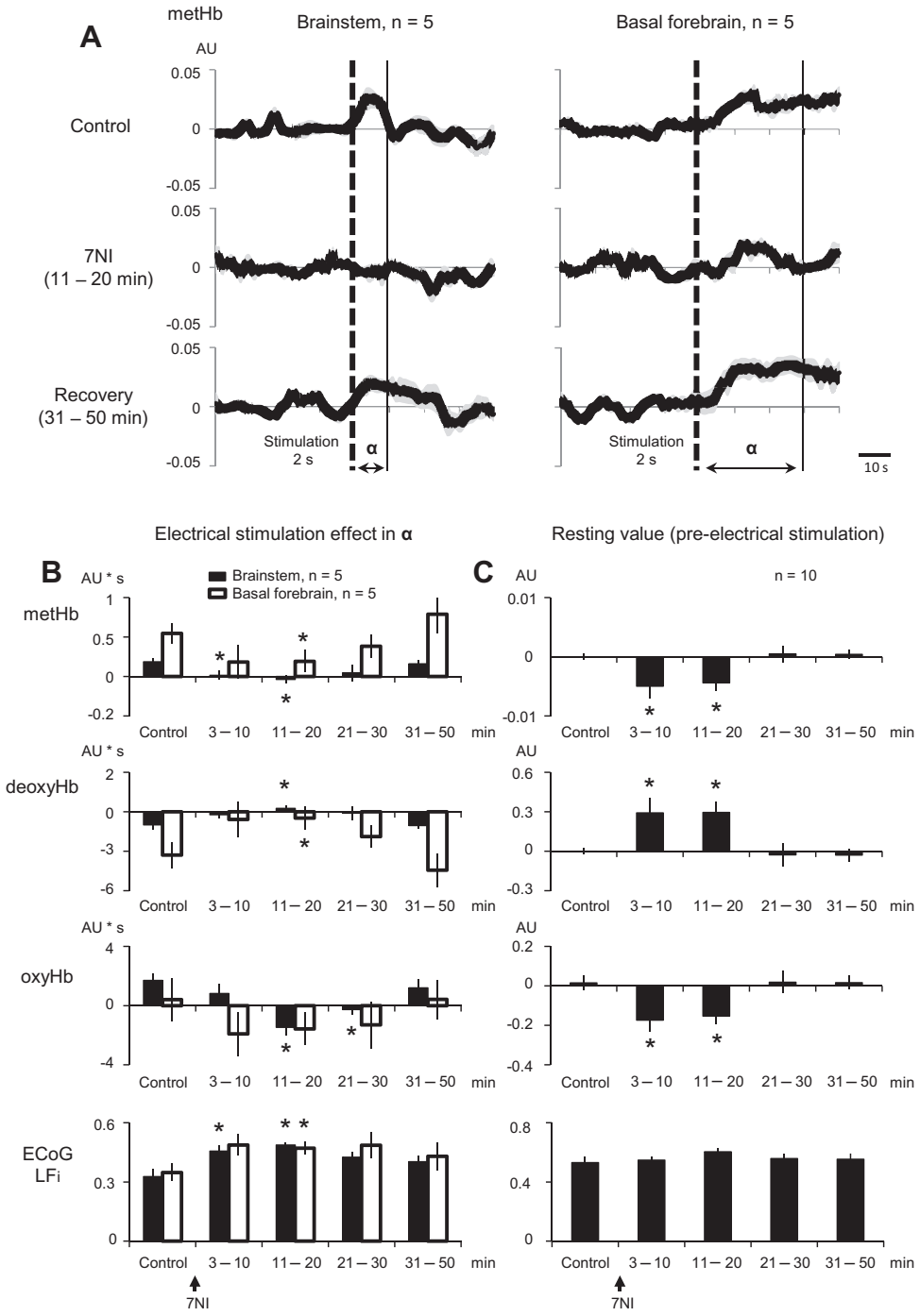

Fig. 4. (A) Effect on metHb before 7NI administration (Control; upper panel), during the peak drug effect (11–20 min after 7NI administration; middle panel) and during recovery (31–50 min; bottom panel) in response to BS (left panel) and BF (right panel) stimulation. Dashed line depicts the electrical stimulation (2 s) and α is the interval of interest. Shaded area denotes SEM for the five recordings obtained from three cats. (B) The area under the curve in α (A) for the three studied markers was compared during control and after 7NI injection for BS (solid bars) and BF (open bars) stimulation. Bottom panel shows the LFi calculated in α. (C) Mean value of metHb and hemodynamic markers before stimulation calculated during control and at different intervals after 7NI injection. Values for BS and BF stimulation were pooled together (n = 10 recordings). Bottom panel shows the LFi before stimulation. Asterisks indicate significant effects compared to control values.

action of NO. For instance, it has been shown that NO may be involved in the NMDA-mediated release of noradrenaline and Glu suggesting that NO can have both direct actions and actions on modulatory processes (Montague et al., 1991). On the other hand previous findings from our group (Cudeiro et al., 1997) obtained with iontophoretic application of 8-bromo-cGMP suggest a simple modulation of the cGMP secondary messenger system. Such an action on cGMP has been widely reported in the literature (for reviews see Garthwaite, 1991; Moncada et al. 1991; Snyder and Bredt, 1991; Schuman and Madison, 1994; Zhang and Snyder, 1995).

In an *in vivo* preparation like the one we used here, it is difficult to clearly separate the NO effects of the vascular and the neuronal compartments. Besides, it has been reported that the exposure of nitrous oxide might interfere with NO metabolism (Zelinski et al., 2009; Ohgami et al., 2010) and with NO background levels. Therefore, we cannot completely exclude a putative interference of the anesthesia with the observed levels of NO, although we trust that our main findings remain, since electrical stimulation produced an increment of NO. In any case, our goal was to discern the participation of neuronal NO in the massive cortical activation induced by the ascendant pathways. The inability of the ascending stimulation to induce such ECoG and metHb changes after the blockage of nNOS clearly points to a direct contribution of the neuronal NO in the activating process.

Possible functional significances of BF and BS activations

Having in mind that the relationship between NO, oxyHb, and deoxyHb is not simple (because the vasodilation induced by NO is also influencing the hemodynamics and the oxy-deoxyHb equilibrium), our work indicates differential actions of both structures (BF and BS) on cortical neurovascular coupling. The present results suggest that changes in cerebral blood flow induced by the basalocortical pathway would be intimately linked to a vasodilation induced by NO. In fact, the monophasic and sustained hemodynamic changes induced by BF stimulation correlate well with the measured NO dynamics, but not with the neuronal activity observed after stimulation. This dissociation between neuronal and hemodynamic activity, previously observed in other brain regions, has been attributed to the participation of inhibitory networks (Ackermann et al., 1984; Buzsaki et al., 2007). The fact that the basalocortical pathway also includes GABAergic fibers supports this hypothesis, allowing a marked hemodynamic change with a less robust response on cortical electrical activity. Previous studies have shown that the BF plays a key role in vigilance states and cognitive functions (Semba, 2000; Jones, 2003, 2004). Because during an attentional process the system must be able to detect and process unexpected signals, a blood flow increase without a dramatic basal neuronal activity disturbance provides sufficient glucose and oxygen for a proper energy metabolism of the neural network.

PBr stimulation, in contrast, involves not only a cortical cholinergic and nitrergic release through BF but also a glutamatergic effect induced via the thalamus that would be the origin of a stronger effect on ECoG as well as the post-stimulus over- and undershoots observed in deoxy- and metHb, respectively. The ability to interfere on cortical activity and the fact that it receives inputs from the lateral parts of the preoptic area (Swanson et al., 1987), an active sleep-promoting structure (Szymusiak and McGinty 1986; Sherin et al., 1996; Szymusiak et al., 2001), supports the hypothesis that the PBr plays a key role in the transitions of the sleep–wake cycle.

Implications in the blood oxygenation level dependent (BOLD) signal interpretation

BOLD signal is a parameter widely used to estimate the cerebral activity which has given rise to functional network maps on several species (Buckner et al., 2008; Pawela et al., 2008; Mantini et al., 2011; White et al., 2011) in virtue of a supposed neurovascular coupling. BOLD response is based on the paramagnetic property of deoxyHb. Thus, changes of deoxyHb concentration in a vascularized area subjected to a magnetic field are reflected as a change in the magnetic resonance (MR) signal. Curiously, neural activity leads to an increase in MR signal even though deoxyHb decreases MR signal (Ogawa et al., 1990). Given the diamagnetic nature of oxyHb, and supported by optical imaging studies (Malonek and Grinvald, 1996), it is believed that this effect occurs because oxyHb displaces deoxyHb that had been suppressing the MR signal intensity. Our data provide a concomitant cause based on the paramagnetic property of metHb being even stronger than deoxyHb. It is due to the fact that unpaired electrons in heme iron of hemoglobin provide paramagnetic properties. Thus, deoxyHb has four unpaired electron and metHb has five (Nitz et al., 2010). As a result, when NO release is associated to a neural activation, a portion of the increase in MR signal might be due to the influence of metHb increase as well. In fact, previous results show an impact of metHb in BOLD response (Duewell et al., 1996; Leung and Moody, 2010, but see Pang et al., 2010) and a recent study has encouraged exploring their clinical implications (Aamand et al., 2013). Finally, we do not discard that other techniques susceptible to high concentrations of metHb, as MR spectroscopy (Gujar et al., 2005), could be affected by NO production.

CONCLUSIONS

The electrical stimulation of the activating ascending systems induces profound changes on cortical (electrical and vascular) activity. We have outlined the role of the neuromodulator NO in this process. Our results reveal a transient cortical increase of the NO marker metHb after the induction of a global brain activation, a change that is abolished after the inhibition of NO synthesis. The present study supports the hypothesis that NO collaborates in the transition from slow-wave sleep to tonic activity in the cortex.

FUNDING

This work was supported by Xunta de Galicia (INCITE09 137 272 PR and Ayudas a Grupos Consolidados).

REFERENCES

Aamand R, Dalsgaard T, Ho YC, Møller A, Roepstorff A, Lund TE (2013) A NO way to BOLD?: Dietary nitrate alters the hemodynamic response to visual stimulation. Neuroimage 83:397–407.

Ackermann RF, Finch DM, Babb TL, Engel Jr J (1984) Increased glucose metabolism during long-duration recurrent inhibition of hippocampal pyramidal cells. J Neurosci 4:251–264.

Bickford ME, Günlük AE, Van Horn SC, Sherman SM (1994) GABAergic projection from the basal forebrain to the visual sector of the thalamic reticular nucleus in the cat. J Comp Neurol 348:481–510.
Buckner RL, Andrews-Hanna JR, Schacter DL (2008) The brain's default network. Ann N Y Acad Sci 1124:1–38.
Buzsaki G, Kalia K, Raichle M (2007) Inhibition and brain work. Neuron 56:771–783.
Cudeiro J, Rivadulla C, Rodríguez R, Grieve KL, Martínez-Conde S, Acuña C (1997) Actions of compounds manipulating the nitric oxide system in the cat primary visual cortex. J Physiol (Lond) 504:467–478.
Cudeiro J, Rivadulla C, Grieve KL (2000) A possible role for nitric oxide at the sleep/wake interface. Sleep 23:829–835.
de Labra C, Rivadulla C, Espinosa N, Dasilva M, Cao R, Cudeiro J (2009) Different sources of nitric oxide mediate neurovascular coupling in the lateral geniculate nucleus of the cat. Front Syst Neurosci 3:9.
Duewell S, Kasserra CE, Jezzard P, Balaban RS (1996) Evaluation of methemoglobin as an autologous intravascular MRI contrast agent. Magn Reson Med 35:787–789.
Feelisch M, Kubitzek D, Werringloer J (1996) The oxyhemoglobin assay. In: Feelisch M, Stamler JS, editors. Methods in nitric oxide research. Chichester: Wiley. p. 455–478.
Francesconi W, Müller CM, Singer W (1988) Cholinergic mechanisms in the reticular control of transmission in the cat lateral geniculate nucleus. J Neurophysiol 59:1690–1718.
Garthwaite J (1991) Glutamate, nitric oxide and cell-cell signalling in the nervous system. Trends Neurosci 14(2):60–67.
González-Mora JL, Martín FA, Rojas-Díaz D, Hernández S, Ramos-Pérez I, Rodríguez VD, Castellano MA (2002) In vivo spectroscopy: a novel approach for simultaneously estimating nitric oxide and hemodynamic parameters in the rat brain. J Neurosci Methods 119:151–161.
Gujar SK, Maheshwari S, Björkman-Burtscher I, Sundgren PC (2005) Magnetic resonance spectroscopy. J Neuroophthalmol 25(3):217–226.
Hartveit E, Ramberg SI, Heggelund P (1993) Brain stem modulation of spatial receptive field properties of single cells in the dorsal lateral geniculate nucleus of the cat. J Neurophysiol 70:1644–1655.
Jones BE (2003) Arousal systems. Front Biosci 8:s438–s451.
Jones BE (2004) Activity, modulation and role of basal forebrain cholinergic neurons innervating the cerebral cortex. Prog Brain Res 145:157–169.
Kelm M, Dahmann R, Wink D, Feelisch M (1997) The nitric oxide/superoxide assay. Insights into the biological chemistry of the NO/O-2 interaction. J Biol Chem 272:9922–9932.
Leung G, Moody AR (2010) MR imaging depicts oxidative stress induced by methemoglobin. Radiology 257:470–476.
Li B, Funke K, Wörgötter F, Eysel UT (1999) Correlated variations in EEG pattern and visual responsiveness of cat lateral geniculate relay cells. J Physiol (Lond) 514:857–874.
Malonek D, Grinvald A (1996) Interactions between electrical activity and cortical microcirculation revealed by imaging spectroscopy: implications for functional brain mapping. Science 272:551–554.
Mantini D, Gerits A, Nelissen K, Durand J-B, Joly O, Simone L, Sawamura H, Wardak C, Orban GA, Buckner RL, Vanduffel W (2011) Default mode of brain function in monkeys. J Neurosci 31:12954–12962.
Mariño J, Cudeiro J (2003) Nitric oxide-mediated cortical activation: a diffuse wake-up system. J Neurosci 23:4299–4307.
Metherate R, Cox CL, Ashe JH (1992) Cellular bases of neocortical activation: modulation of neural oscillations by the nucleus basalis and endogenous ACh. J Neurosci 12:4701–4711.
McCormick DA, Bal T (1997) Sleep and arousal: thalamocortical mechanisms. Annu Rev Neurosci 20:185–215.
Moncada S, Palmer RM, Higgs EA (1991) Nitric oxide: physiology, pathophysiology, and pharmacology. Pharmacol Rev 43(2):109–142.
Montague PR, Gancayco CD, Winn MJ, Marchase RB, Friedlander MJ (1991) Role of NO production in NMDA receptor-mediated neurotransmitter release in cerebral cortex. Science 263(5149):973–977.
Moruzzi G, Magoun HW (1949) Brain stem reticular formation and activation of the EEG. Electroencephalogr Clin Neurophysiol 1:455–473.
Nitz WR, Balzer T, Grosu DS, Allkemper T (2010) Principles of magnetic resonance. In: Reimer P, Parizel PM, Meanev JFM, Stichnoth F-A, editors. Clinical MR imaging: a practical approach. Springer.
Ogawa S, Lee TM, Nayak AS, Glynn P (1990) Oxygenation-sensitive contrast in magnetic resonance image of rodent brain at high magnetic fields. Magn Reson Med 14:68–78.
Ohgami Y, Chung E, Quock RM (2010) Nitrous oxide-induced NO-dependent neuronal release of β-endorphin from the rat arcuate nucleus and periaqueductal gray. Brain Res 1366:38–43.
Pang KK, Tsai YS, Chang HC, Hsu KN (2010) Methemoglobin suppression in a 0.3 Tesla magnet: an in vitro and in vivo study. Acad Radiol 17(5):624–627.
Pawela CP, Biswal BB, Cho YR, Kao DS, Li R, Jones SR, Schulte ML, Matloub HS, Hudetz AG, Hyde JS (2008) Resting-state functional connectivity of the rat brain. Magn Reson Med 59:1021–1029.
Rivadulla C, de Labra C, Grieve KL, Cudeiro J (2011) Vasomotion and neurovascular coupling in the visual thalamus in vivo. PLoS One 6:e28746.
Schuman EM, Madison DV (1994) Nitric oxide and synaptic function. Annu Rev Neurosci 17:153–183.
Semba K (2000) Multiple output pathways of the basal forebrain: organization, chemical heterogeneity, and roles in vigilance. Behav Brain Res 115:117–141.
Sherin JE, Shiromani PJ, McCarley RW, Saper CB (1996) Activation of ventrolateral preoptic neurons during sleep. Science 271:216–219.
Snyder SH, Bredt DS (1991) Nitric oxide as a neuronal messenger. Trends Pharmacol Sci 4:125–128.
Steriade M, Paré D, Parent A, Smith Y (1988) Projections of cholinergic and non-cholinergic neurons of the brainstem core to relay and associational thalamic nuclei in the cat and macaque monkey. Neuroscience 25:47–67.
Steriade M, Dossi RC, Nuñez A (1991a) Network modulation of a slow intrinsic oscillation of cat thalamocortical neurons implicated in sleep delta waves: cortically induced synchronization and brainstem cholinergic suppression. J Neurosci 11:3200–3217.
Steriade M, Dossi RC, Paré D, Oakson G (1991b) Fast oscillations (20–40 Hz) in thalamocortical systems and their potentiation by mesopontine cholinergic nuclei in the cat. Proc Natl Acad Sci U S A 88:4396–4400.
Steriade M, Amzica F, Nuñez A (1993a) Cholinergic and noradrenergic modulation of the slow (approximately 0.3 Hz) oscillation in neocortical cells. J Neurophysiol 70:1385–1400.
Steriade M, McCormick DA, Sejnowski TJ (1993b) Thalamocortical oscillations in the sleeping and aroused brain. Science 262:679–685.
Steriade M, Jones EG, McCormick DA (1997) Thalamus. Organization and function, vol. 1. Oxford: Elsevier. p. 269–337.
Swanson LW, Mogenson GJ, Simerly RB, Wu M (1987) Anatomical and electrophysiological evidence for a projection from the medial preoptic area to the 'mesencephalic and subthalamic locomotor regions' in the rat. Brain Res 405:108–122.
Szymusiak R, McGinty D (1986) Sleep-related neuronal discharge in the basal forebrain of cats. Brain Res 370:82–92.
Szymusiak R, Steininger T, Alam N, McGinty D (2001) Preoptic area sleep-regulating mechanisms. Arch Ital Biol 139:77–92.
Uhlrich DJ, Tamamaki N, Murphy PC, Sherman SM (1995) Effects of brain stem parabrachial activation on receptive field properties of cells in the cat's lateral geniculate nucleus. J Neurophysiol 73:2428–2447.
Wolfe J, Palmer LA (1998) Temporal diversity in the lateral geniculate nucleus of cat. Vis Neurosci 15:653–675.

White BR, Bauer AQ, Snyder AZ, Schlaggar BL, Lee J-M, Culver JP (2011) Imaging of functional connectivity in the mouse brain. PLoS One 6:e16322.

Zelinski LM, Ohgami Y, Quock RM (2009) Exposure to nitrous oxide stimulates a nitric oxide-dependent neuronal release of beta-endorphin in ventricular-cisternally-perfused rats. Brain Res 1300:37–40.

Zhang J, Snyder SH (1995) Nitric oxide in the nervous system. Annu Rev Pharmacol Toxicol 35:213–233.

Zijlstra WG, Buursma A, Assendelft OW (2000) Visible and near-infrared absorption spectra of human and animal hemoglobin: determination and application. Zeist, Netherlands: VSP.

(Accepted 17 November 2014)
(Available online 25 November 2014)